OBTAINING METAL-CERAMIC LAYERS BY LASER CLADDING USING ALUMINA POWDER MIXTURES

S. Mihai[1], D. Chioibasu[1], A. C. Popescu[1], S. Craciun[2], V. Geanta[3], R. Stefanoiu[3], I. Voiculescu[2]*

[1]National Institute for Laser, Plasma and Radiation Physics, Center for Advanced Laser Technologies,077125 Ilfov, Romania
[2]National University of Science and Technology POLITEHNICA Bucharest, Faculty of Industrial Engineering and Robotics, 060042 Bucharest, Romania
[3]National University of Science and Technology POLITEHNICA Bucharest, Faculty of Science and Engineering of Materials, 313 Splaiul Independentei, 060042 Bucharest, Romania
*Corresponding author's e-mail address: craciunstefan98@gmail.com

ABSTRACT

This paper presents a comparative analysis of the metal-ceramic powders mixtures behaviour deposited onto 304 stainless steel (SS304) substrate by laser procedure. Using Inconel 718 (In718) alloy as a matrix material that has a lower melting range in comparison with the austenitic stainless steel, a more reduced overheating phenomenon of the cladding layer has been achieved for the same values of the laser deposition parameters. On the other hand, due to the greater fluidity of the In718 alloy, comparing to the SS304 material, an increase of the cladded layer width has been observed at the macro and microstructure analysis. Moreover, an improvement of the adhesion phenomenon between the cladded layer and the substrate was found when spherical alumina (Al_2O_3) particles have been used. The comparative analysis of the results in case of metal matrix composite (MMC), which was developed by mixing different percentages of Al_2O_3, SS304 or In718, has revealed that the laser power of 500W and cladding speed of 10mm/s are the optimal process parameters.

KEYWORDS: Laser cladding, ceramic, alumina, powder mixtures, microstructure

1. INTRODUCTION

The Al_2O_3 - based ceramics present outstanding properties, such as corrosion and high-temperature oxidation resistance [1]-[3], that make them a suitable composite material for the aero engine applications [4]. Besides, the manufacturing process that can be applied to achieve the complex structure and refined microstructure of melt-grown Al_2O_3-based ceramics has tremendous development potential [5]-[8].

Additive manufacturing method, like laser directed energy deposition (LDED) technology, can be employed to achieve one-step near-net fabrication of complex shape parts [9]-[11]. During the LDED process, due to the fast heating-cooling process, the deposited material suffers modification of metallurgical properties that has a crucial influence on the material mechanical properties.

However, because of the opacity of the molten pool and fastness of melting and solidification processes, the detection and observation of the phenomena in real time could be considered a challenge for the researchers [12]. Due to the development of software and know-how in computer science, the modelling and numerical simulation have become a useful tool for prediction and analysis of the solidification process evolution [13].

Some researchers have successfully prepared almost full-dense Al2O3-based ceramics by LDED, such as Al_2O_3/ZrO_2, $Al2O_3$/YAG, and Al_2O_3/YAG/ZrO_2 [14-16]. Liu et al. [17] have performed the manufacture of large-size rod-like and irregular-shaped $Al_2O_3/GdAlO_3/ZrO_2$ eutectic ceramics, demonstrating the potential of LDED technology for preparing Al2O3-based ceramics. However, the mechanical properties of Al_2O_3-based ceramics, such as microhardness, fracture toughness, and flexural strength, have always been a concern in the LDED manufacturing process fabricated [18].

Due to the finer solidification microstructure, it was reported that the mechanical properties of Al2O3-based ceramics fabricated by LDED are not superior to those of ceramic samples which have been prepared by sintering and other solidification methods [19]-[21]. More precisely, because during the solidification process, defects like pores and cracks may be

Date of submission/acceptance: 31.05.2024/15.12.2024
http://doi.org/10.35219/awet.2024.02

developed, the flexural strength is relatively low [18]. Consequently, being one of the methods that can be applied for achieving new high-temperature structural materials, it is necessary to develop new investigations on the relationship between solidification defects and fracture behaviour of Al_2O_3-based ceramics manufactured by LDED [20]-[25]. One of the objectives of the research was to analyse the influence on the coated layers microstructure, deposited by LDED, of the ceramic powders' concentration from the metal-ceramic mixtures with different percentages of Al_2O_3, SS304 and In718 powders. Also, a comparative analysis of the microstructure and morphology of the cladded layers determined by the temperature reached during laser melting of powder mixtures was made in detail. It was found that in case of using SS304 or In718 metal powders, with additions of 10% Al_2O_3, for the same values of the LDED parameters, the cracking phenomenon may be developed when the layers overlap was up to 30%.

2. MATERIALS AND METHODS

2.1. Materials

The materials selected to obtain the metal-ceramic layers were alumina powders (Al_2O_3) mixed with metal powders SS304 and In718 alloy whose morphology is presented in figure 1. They were deposited by laser cladding on a substrate of high-alloy steel SS 304 having in composition the following chemical elements (wt.%): C - 0.08; Mn - 2; Si - 0.75; P - 0.045; S - 0.03; Cr - 20; Ni - 10.5; Fe - bal.

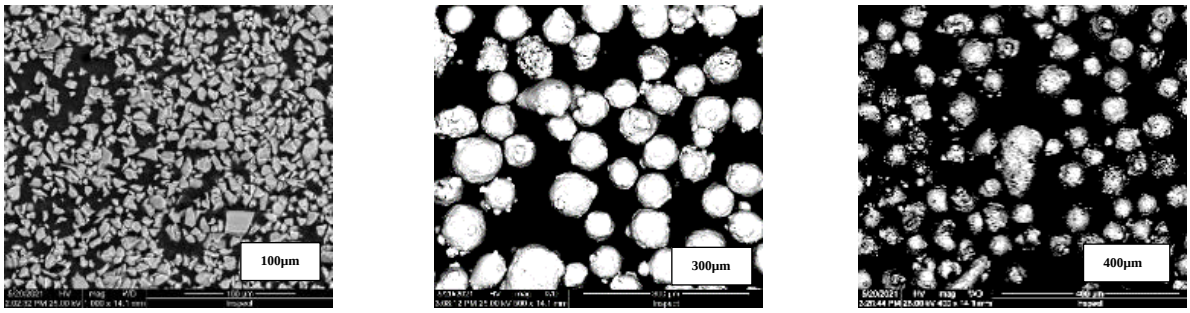

a) b) c)

Fig. 1. Powders used to obtain metal-ceramic layers on SS304 substrate: a) Al_2O_3; b) In718; c) SS304

The pure ceramic alumina (99%) (Sigma-Aldrich, Darmstadt, Germany), used in powder form with polyhedral particles of about 20µm, was mixed in different percentages with the following powders:

- *In718* (Höganäs AB, Sweden), as spherical particles powder with 45-90µm dimension, having the following chemical composition (wt.%): Ni - 52.8; Cr - 19.2; Fe - 18.18; Nb - 5; Mo - 3; Ti - 1; Al - 0.6; Si< 0.10 Si; C - 0.05; Mn - 0.02; Ta<0.01; Cu<0.01; N - 0.006; P - 0.005; S - 0.003; B - 0.002;
- *SS304* with 45-100 µm grain size and the following chemical composition (wt.%): C - 0.08; Mn - 2; Si - 0.75; P - 0.045; S - 0.03; Cr - 20 Cr; Ni - 10.5 Ni; Fe - bal.

Before starting the deposition welding process, the powder mixtures were homogenized by employing a mechanical system with balls (model S100, Retsch, United Kingdom) and Ar, as shielding gas, for four hours, at speed of 200rpm.

2.2. Methods

The metal-ceramic layers were linearly deposited by LDED, without or with layers overlap up to 30%. The melting process parameters were adjusted, so that the volume unmelted material to be as reduced as possible. The coated surfaces with section of 15x40 mm^2 have been carried out on SS304 substrate that has 5x100x100mm and 10x100x100mm dimensions.

The process was carefully monitored, in order to perform deposits with dense structure, good adhesion to the substrate, reduced oxidation and non-uniformity.

The melting laser deposition experiments were carried out by employing an integrated system that comprises the laser source, robotic system and processing optics. The laser is Yb:YAG, TruDisk 3001 (Trumpf, Germany), operating in continuous mode, with a wavelength of λ = 1030 nm and a maximum power of 3 kW. The laser beam is transferred through the optical fiber to the focusing system, BEO D70 (Trumpf, Germany) that is positioned on a robotic arm Kr30HA (Kuka, Germany) with six degrees freedom (6 DOF). The SS304 plates, having the role of substrate, were degreased with ethyl alcohol and dried with compressed air. The powders were combined with isopropanol in 3:1 ratio, to create a slurry that was, subsequently, applied on the substrate. To protect the laser optics and prevent the oxidation phenomenon, the cladding process was made in Ar 5.0 shielding gas with ultra-high purity (99.99%). To ensure the uniformity and the same hight of the powder material on the whole surface, it was used a levelling device, as it can see in figure 2a.

The diameter of the laser spot was determined by measuring the size of the imprint printed on the anodized Al control sample, having focus of 0.8 mm in, at 16 mm from the level of the surface to be processed (fig. 2b).

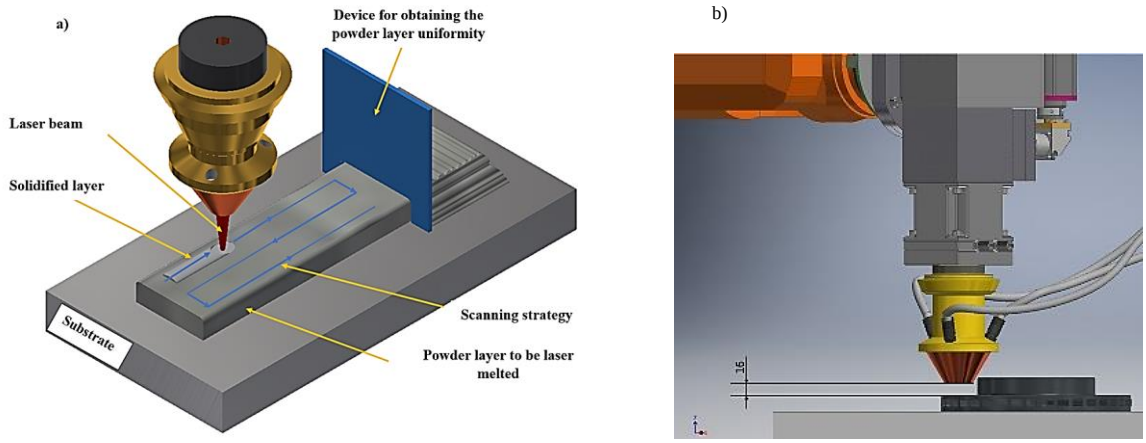

Fig. 2. Laser cladding: a) process principle; b) positioning of processing optics

To determine the optimal laser processing parameters, several deposition trials with the composite material, having different concentrations of the ceramic material (100, 83, 71, 62, 10 and 5%) were performed with different laser beam powers (1000-15000 W). For all deposited layers, the height of the powder layer was about 0.45mm, and a cladding speed of 5mm/s was maintained constant during the whole melting process. To monitor the modification of temperature in the area irradiated by the laser beam, a thermal imaging camera (TIM M-05, Micro-Epsilon, Germany), capable of recording temperature in the range of 900-2450°C, was employed in the experimental programme.

The temperature distribution in the laser-irradiated area was recorded using resolution of 382x288 pixels (pixel size ~330 μm) and frequency of 80 Hz, being characteristic to the mode of 80 frames per second. The camera was positioned at distance of about 60 cm from the irradiated surface and covered an approximative area of 25x15cm^2. For assessing the quality of the cladded layers, the samples were cut with a precision cutting saw (ISOMet 4000, Dusseldorf, Germany).

Further, the samples were prepared by grinding and polishing techniques with a precision machine Buehler (Germany) and metallographic abrasive materials (abrasive papers with progressive grain from 240 to 600μm; aluminium oxide polishing suspension of pH 7 and diameter from 1 to 0.25μm). After etching the surfaces with Kroll metallographic reagent, the examination of the microstructure in the cross-section of samples was carried out with the optical microscope (Olympus GX51, Tokyo, Japan).

3. RESULTS AND DISCUSSION

3.1. Laser Cladding

Two laser cladding technologies and different mixtures of ceramic powders were designed and developed in the experimental programme. Based on the comparative analysis of the deposits performed with different ratios of the ceramic powder, it was found that the main parameters - laser power, deposition speed, layers overlap – have crucial influence on the quality and aspects of the cladded layers.

Table 1 shows the preliminary process parameters, in association with different mixtures of polyhedral Al_2O_3, SS304 and In718 spherical powders, used as metallic matrix, applied for optimizing the laser cladding process. For laser power of 1000W and low concentrations of ceramic powder (5 or 10% Al_2O_3), uniform and parallel depositions, with well-defined edges, were obtained. When higher composition of ceramic powder was used, partially melted areas, uneven appearance, and reduced adhesion of cladded layer to the high-alloy steel substrate were observed.

Based on the visual control of the cladded layers, it was found that the optimal coating conditions are the following: maximum 10%Al_2O_3 ceramic powder dispersed in 90%SS304 metal matrix, laser power of 1000W and cladding speed of 5mm/s. On the contrary, reduced adhesion of the layer to the substrate, continuous and coagulated deposit in the structure of the layer and uneven edges were found when the mixture of powders contained 5 or 10% Al_2O_3 and 95 or 90% In718.

As it can be seen in figure 3, smooth and uniform aspect of the cladded layer is associated with using metal powders in proportion of 100% (Fig. 3 e and f), while wavy edges and inhomogeneous aspect are observed when the Al_2O_3 was added in the powders mixture (Fig. 3a - Fig.3d).

During cladding process, the temperature modifications were recorded and plotted, as figure 3 shows. The software allows collecting quickly and easy the temperature data and, further, plotting the temperature versus time profile, with great accuracy. For easier tracking of the temperature variation, different intensity levels have been assigned to false colours in order to highlight the limits of values.

Table 1. Preliminary parameters applied for laser cladding process using a mixture of metal-ceramic powders

Sample No.	Deposition strategy	Power [W]	Velocity [mm/s]	Powder layer height[mm]	Powder composition [%]	Aspect of cladded layers
P1	line	1000	5	0.45	100% Al2O3	Discontinuous deposition, islands of molten material separated from unmelted powder
P2	line	1000	5	0.45	100% Al2O3	Discontinuous deposition, islands of molten material separated from unmelted powder
P3	line	1500	5	0.45	100% Al2O3	Discontinuous deposition, islands of molten material separated from unmelted powder
P4	line	1000	5	0.45	85% Al2O3 15% SS304	Excess unmelted powder, that can easily be removed from the substrate
P5	line	1000	5	0.45	71% Al2O3 29% SS304	Excess unmelted powder, that can easily be removed from the substrate
P6	line	1000	5	0.45	62% Al2O3 38% SS304	Excess unmelted powder, that can easily be removed from the substrate
P7	line	1000	5	0.45	10% Al2O3 90% SS304	Coagulated continuous deposition in the central area of the spot, blurred edges
P8	line	1000	5	0.45	5% Al2O3 95% SS304	Coagulated continuous deposition in the central area of the spot, blurred edges
P9	line	1000	5	0.45	10% Al2O3 90% In718	Coagulated continuous deposition in the central area of the spot, blurred edges
P10	line	1000	5	0.45	5% Al2O3 95% In718	Coagulated continuous deposition in the central area of the spot, blurred edges
P11	line	1000	5	0.45	100% In718	Continuous deposition of material with well-defined and parallel edges
P12	line	1000	5	0.45	100%SS304	Well-defined edge deposition of material with well-defined and parallel edges
P13	Meander, overlap of 30%	1000	5	0.45	10% Al2O3 90% SS304	Continuous deposition of material with well-defined and parallel edges
P14	Meander, overlap of 30%	1000	5	0.45	10% Al2O3 90% In718	Solidified layers with reduced adhesion to the substrate
P15	Meander, overlap of 22%	1000	5	0.45	10% Al2O3 90% In718	Solidified layers with cracks
P16	Meander, overlap of 22%	1000	5	0.45	10% Al2O3 90% SS304	Continuous deposition of material with well-defined and parallel edges, with cracks

The recorded thermograms can provide significant information about the dynamics of the liquid phase, the adhesion between the layers and substrate, as well as on the thermal gradient of the molten pool, that can allow the identification of the potential sources of defects, such as pores, cracks or structures with inhomogeneous composition (Fig. 4). For instance, the higher temperatures (T_{max}) correspond to the overheating phenomenon and to increasing the fluidity of the molten material, while the lower temperatures (T_{min}) correspond to the phenomena associated with phase transformation or incomplete melting of the powder mixture.

Based on the preliminary results, a second set of experiments was designed and another type of material, pure alumina (99.9%) (Wellion Trade Company, Taiwan), consisting in spherical particles with 45-90μm size, was mixed in different percentages with SS304 powder (Höganäs AB, Sweden), having spherical particles with 45-106μm size and the following composition (wt%): C - 0.08; Mn - 2; Si - 0.75; P - 0.045; S - 0.03; Cr - 20; Ni - 10.5; Fe – bal.).

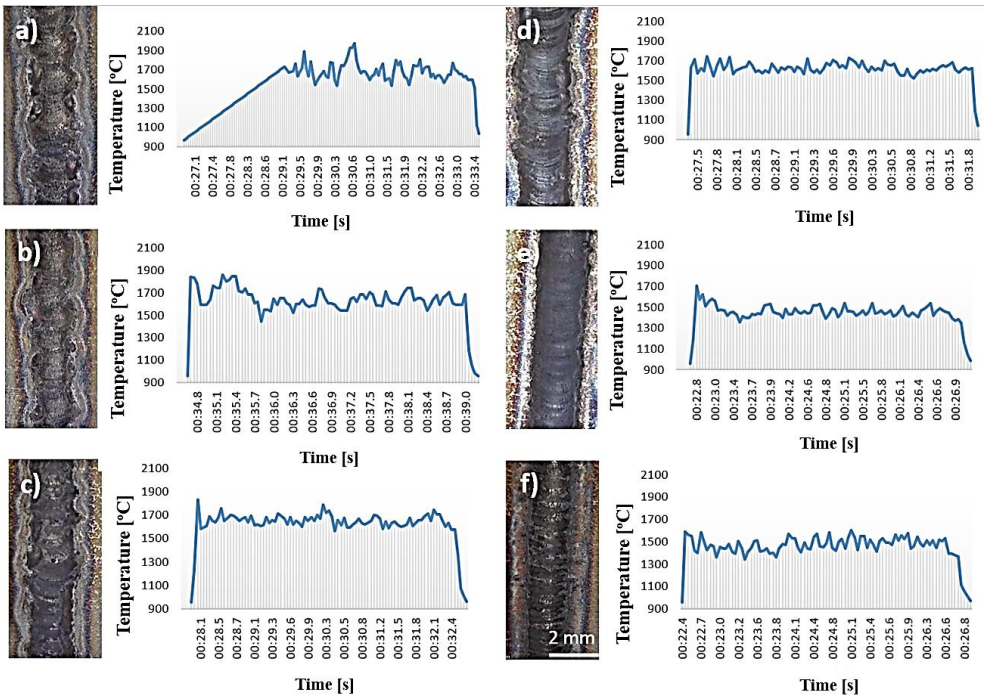

Fig. 3. Macroscopic appearance of laser deposits and the corresponding thermograms:
a) SS304 + 10%Al2O3; b) SS304 + 5%Al2O3; c) In718 + 10%Al2O3; d) In718 + 5%Al2O3; e) In718; f) SS304

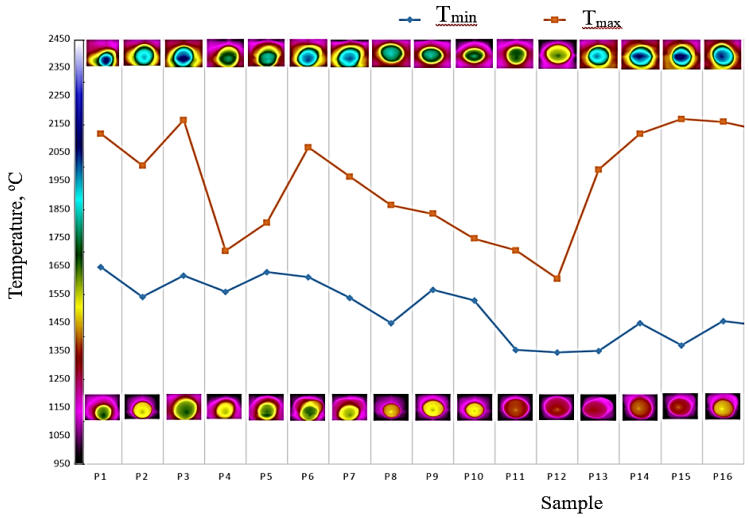

Fig. 4. Temperature range recorded during laser cladding

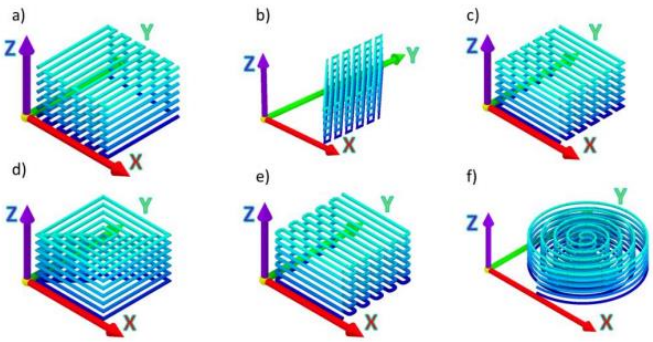

Fig. 5. Scanning strategies used to optimize laser deposition and metal-ceramic powder mixtures:
meander (a, c, e), inclined meander (b), contour (d) and spiral (f)

The main goals of the research were focused on solving two technical issues: ensuring better adhesion of the deposit to the metal substrate, and reducing the laser processing temperature. Applying various power values (300W - 1200W) and scanning speeds (5mm/s - 10mm/s), a powder mixture with height of 0.45mm has been melted on a SS304 steel substrate. Further, the MMC composite, compounded of SS304 + 30%Al_2O_3, has been melted so that overlapping the trajectory lines from 30% to 45%, several tens of mm^2 coated surfaces to be obtained. This stage was important in optimizing the laser processing parameters and for determining the overlapping parentage so that a larger coated area to be carried out. Finally, the best results were found when the trajectory lines generated through the scanning strategy overlap in percentage of 30% (Fig. 5).

As it is shown in figure 6, the main issues that may occur during laser cladding with powder mixtures are the accumulation of powder material, uneven coverage of the substrate, oxidation of the deposited metal layer, excess of unmelted material, and cracks. The fast melting, cooling and solidification of the molten metal may often generate local stress that can cause initiation and propagation of cracks. Moreover, it was noticed that addition ceramic in metal matrix could frequently lead to development of cracks. According to the information presented in table 1, crack-free samples can be achieved when layers overlap is 30%and only 10% Al_2O_3 is added in the metal powder mixture (samples P13 and P14). Also, based on the thermal images, the laser cladding conditions which determine the unstable and stable melting process have been identified, as figure 7 displays. In the table 2 the optimal laser cladding parameters are centralized, being associated to the metal-ceramic powder mixtures melted on the stainless steel substrate. The experiments aimed to obtain uniform deposits, without interface discontinuities and defects like pores or cracks in the structure of the cladded layers.

However, the main issue that needs attention in the optimization of cladding parameters is the different behaviour of materials in terms of absorbing the energy developed by the laser beam. While the spherical alumina particles absorb partially the heat generated by the laser beam, the metallic material reflects partially the energy or uses it for fast melting, allowing inclusion of ceramics within the deposits. It was found that higher values of laser power can determine local vaporization of the metallic material, generating pores in the deposition volume. On the other hand, lower values of laser power may lead to incomplete melting of the powder mixture, causing poor resistance to cracking and weak adhesion of the cladded layer to the substrate [26].

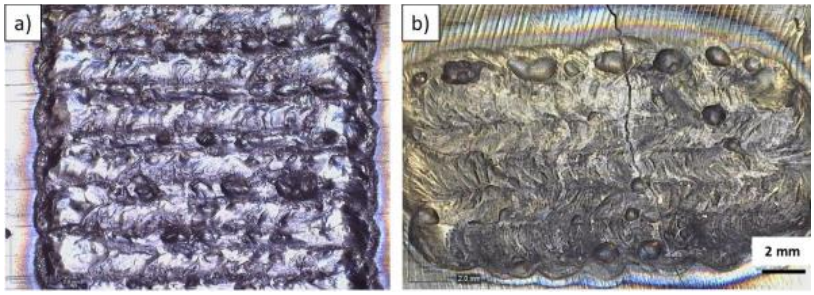

Fig. 6. Image of laser cladded surfaces: a) compliant deposits; b) non-compliant deposits with cracks

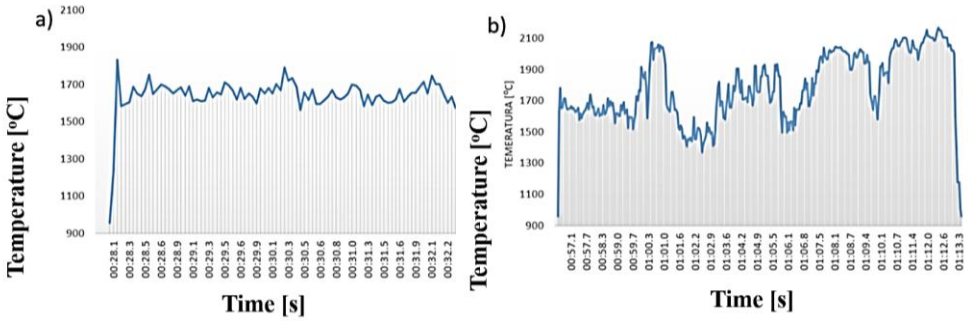

Fig. 7. Comparative analysis of temperature variation during laser cladding with powder mixtures: a) stable melting process; b) unstable melting process

3.2. Microstructure

The microstructures of cladded samples performed with the first set of parameters are shown in figure 8, in concordance with the information presented in table 1. If the process temperature was slightly above the melting temperature of Al_2O_3 (2072°C), high penetration, inclusion of ceramic powder and wavy edges were observed (P1, Fig. 8a). On the other hand, if the laser power increased to 1500W, the penetration did not significantly modify, but a flattening and widening of the deposit was noticed (P3, Fig. 8b).

Table 2. Optimal laser cladding parameters associated to the metal-ceramic mixtures used

Sample No.	Scanning strategy	Laser Power [W]	Laser speed [mm/s]	Layer height [mm]	Powder composition
S1	Line	1000	5	0.45	10% Al_2O_3 + 90% SS
S2	Line	1000	5	0.45	15% Al_2O_3 + 85% SS
S3	Line	1000	5	0.45	20% Al_2O_3 + 80% SS
S4	Line	1000	5	0.45	25% Al_2O_3 + 75% SS
S5	Line	1000	5	0.45	30% Al_2O_3 + 70% SS
S6	Line	1000	5	0.45	40% Al_2O_3 + 60% SS
S7	Meander	1000	15	0.45	40% Al_2O_3 + 60% SS
S8	Meander	1000	10	0.45	40% Al_2O_3 + 60% SS
S9	Meander	1000	10	0.45	40% Al_2O_3 + 60% SS
S10	Meander	1000	10	0.45	40% Al_2O_3 + 60% SS
S11	Meander	1200	10	0.45	40% Al_2O_3 + 60% SS
S12	Line	600	10	0.45	40% Al_2O_3 + 60% SS
S13	Line	600	10	0.45	30% Al_2O_3 + 70% SS
S14	Line	400	10	0.45	30% Al_2O_3 + 70% SS
S15	Line	400	10	0.45	40% Al_2O_3 + 60% SS
S16	Meander	400	10	0.45	30% Al_2O_3 + 70% SS
S17	Meander	400	10	0.45	30% Al_2O_3 + 70% SS
S18	Meander	400	10	0.45	30% Al_2O_3 + 70% SS
S19	Meander	300	10	0.45	30% Al_2O_3 + 70% SS
S20	Meander	500	10	0.45	30% Al_2O_3 + 70% SS

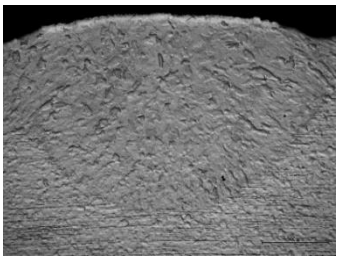
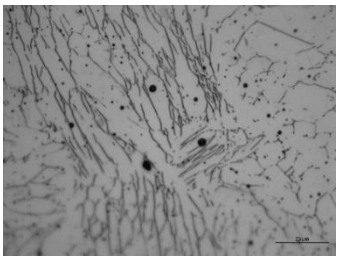

a) Sample P1 (100% Al_2O_3, laser power of 1000W): Substrate remelting and detail on austenite matrix, containing delta ferrite network, finely dispersed inter-metallic compounds, pores and reduced amount of embedded alumina

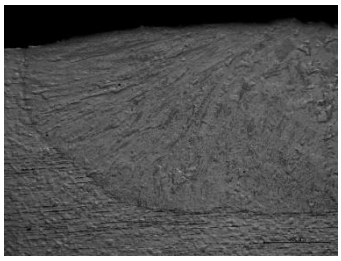

b) Sample P3 (100% Al_2O_3, laser power of 1500W): SS304 Substrate remelting

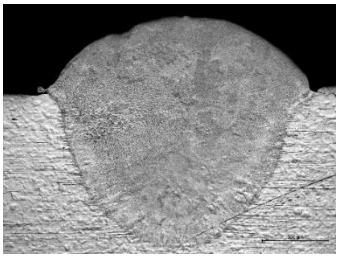
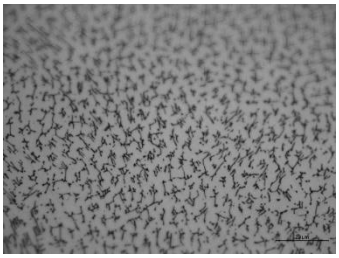

c) Sample P4 (83% Al_2O_3 + 17% SS304): Deposit with high overlap and detail on austenite matrix, containing delta ferrite network and reduced inclusion of alumina particles

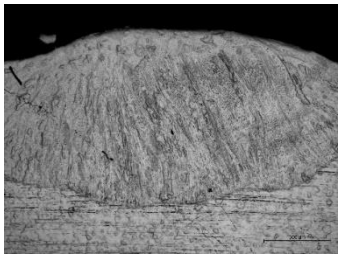

d) Sample P9: 10% Al_2O_3 + 90% In718

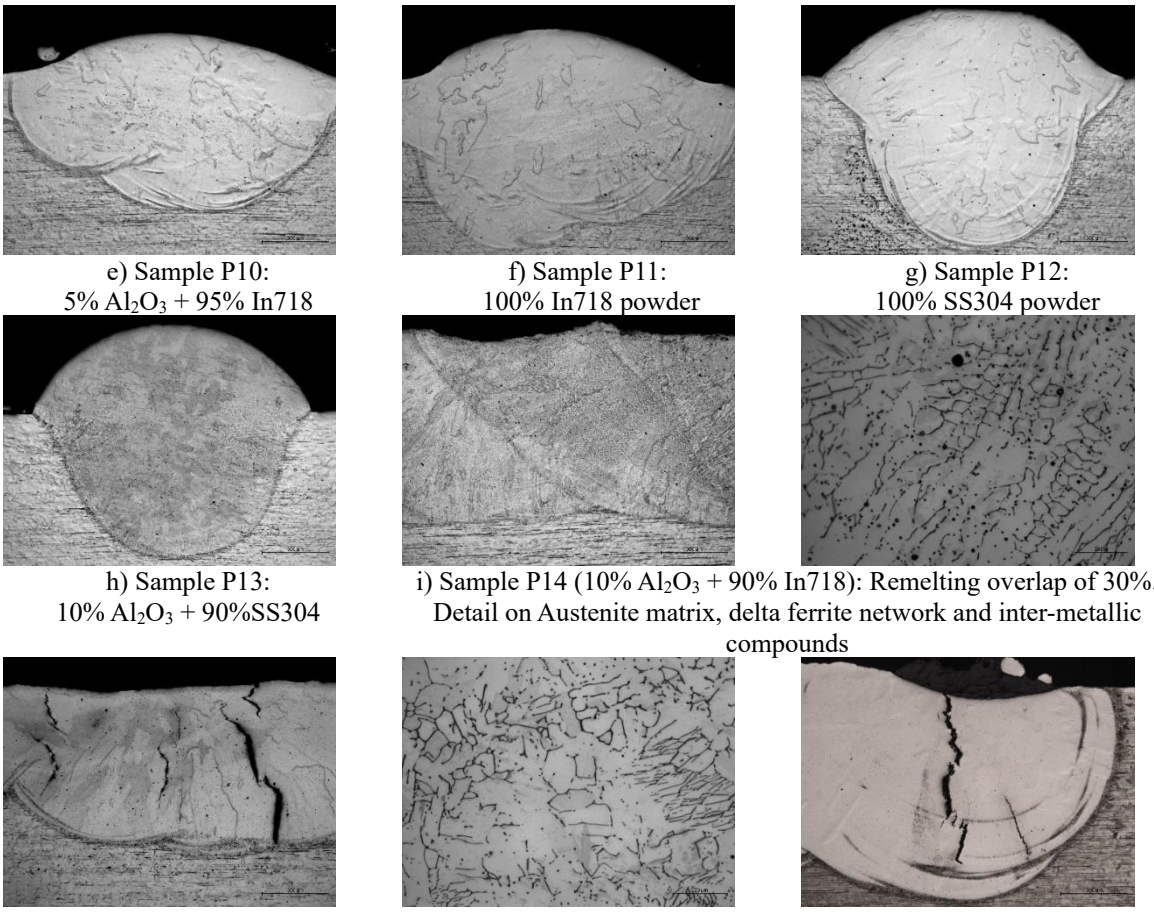

e) Sample P10: 5% Al_2O_3 + 95% In718

f) Sample P11: 100% In718 powder

g) Sample P12: 100% SS304 powder

h) Sample P13: 10% Al_2O_3 + 90%SS304

i) Sample P14 (10% Al_2O_3 + 90% In718): Remelting overlap of 30%. Detail on Austenite matrix, delta ferrite network and inter-metallic compounds

j) Sample P15 (10% Al_2O_3 + 90% In718, overlap of 22%. Detail on Austenite matrix, delta ferrite network and large inter-metallic compounds

k) Sample P16 (overlap of 22%) 10% Al_2O_3 + 90% SS304

Fig. 8. Cross-sections macro and microstructures of laser cladded layers

If the input heat is insufficient to melt the alumina (dosed in 85% percentage), and the temperature range (T_{max}-T_{min}) is too narrow (1550-1700°C), the melting of powders mixture can be incomplete (P4, Fig. 8c). Using a powders mixture of In718 and Al_2O_3, it was found an improvement of the deposits quality (P9, P10, Fig. 8d and Fig. 8e), due to an adequate wetting of the ceramic material determined by high Ni content, and higher temperatures (1750-2100°C) that ensure the appropriate melting and the fluidity increase of the metal alloy (In718 has melting temperature range of 1260-1336°C). Besides, lower overheating and the increase of the deposit width have been observed in case of samples P9 and P10. If the percentage of In718 increases at 100%, the appearance of the deposit is aesthetically better (P11, Fig. 8f).

Using 100% SS304, the lower melting temperature (1400-1450°C) of the powder has determined adherent and homogeneous deposits, with higher height, comparing to the In718 alloy (P12, Fig. 8g). A good aspect of the cladded layers was also noticed in case of SS304 with Al_2O_3 mixture (P13, Fig. 8h), the deposited layer having a larger reinforcement.

When the depositing path followed a meandering trajectory, with an overlap of about 30% of the layers, the appearance of the coated surface was less aesthetic in case of 10% Al_2O_3 + 90% In718 powders mixture, but without unacceptable imperfections and defects, (P14, Fig. 8i). If the overlapping degree decreases at 22%, both in In718 and in SS304 mixture, cracks have been observed, as it can be noticed in figure 8j and figure 8k. The cracks found in the samples P15 and P16 were developed during the cladding process, the main cause being the stress field generated by solidification, followed immediately by remelting and overlapping of layers. This phenomenon could be associated to the overlapping value of 22% that seems to be insufficient in terms of the solidification stress balancing.

The high temperature, reached during the melting of powders mixture, has determined the complete melting of the alumina, and, subsequently, the formation of fusible compounds that have inter-dendritically segregated. During the cooling phase, these fusible compounds have solidified later than the metallic matrix, this phenomenon being the main cause of tensile stress development, and, finally, of initiation and propagation of cracks in the deposited layers. Because the cracking direction is identical with the growth direction of dendrites, it is obvious that the cracks are developed by hot cracking mechanism.

The chemical analysis of the high-entropy alloy (HEA) substrate provided information on the chemical elements (wt.%), as follows: Al - 6.68 %; Co - 24.36%; Cr - 21.47%; Fe - 23.12%, and Ni - 24.36%.

After ending the laser cladding, the cross sections were prepared by metallographic technique, being etched with Kroll reagent in order to be examined by SEM method (Inspect Quanta microscope, FEI, Netherlands equipped with Ametec Z2e chemical composition analyser). It was found that the deposit made by laser cladding of 30% Al_2O_3 + 70% SS304 powders mixture with 500W laser power is homogeneous, has a good adherence to the substrate, and contains fine needle-like dendrites oriented on the heat flow direction (Sample 20, Table 2, Fig. 9).

As figure 10 exhibits, a mixing zone of about 20µm width was developed between the cladded layer and the high-entropy alloy substrate. Besides, the cladded layer - substrate interface is continuous, without imperfections, and a diffusion phenomenon of chemical elements from one material to another and vice versa has appeared in this area.

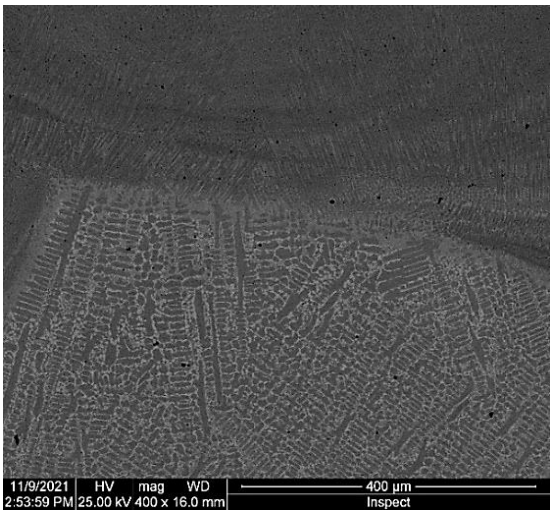

Fig. 9. Cross-sectional SEM images of sample 20

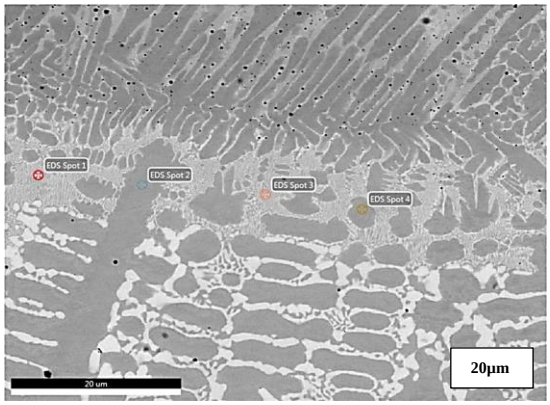

Fig. 10. Detail on the transition zone from cladded layer to substrate

In the heat affected zone, a slight grain growth has occurred, without altering the phase ratio. The EDS micro-chemical composition analysis revealed higher percentage of Co in the bonding area, the effect being explained by the mixture of cladded layer with the substrate that contains Co in composition (Fig. 11).

Figure 12 shows the distribution of chemical elements along a line crossing the interface between the HEA alloy substrate and the deposited layer made by cladding laser of metal-ceramic powders mixture. On the distance of about 90µm, on either side of the interface, a quasi-constant percentage of chemical elements is observed in both materials, excepting the Fe element that is present in the chemical composition of the SS304 material (Fig. 12).

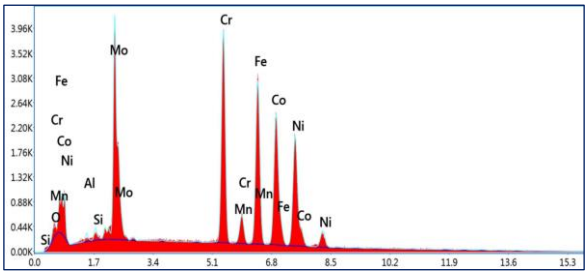

a)

Element	Weight %	Atomic %	Net Int.	Error %
O K	0.50	1.88	5.43	27.76
AlK	0.58	1.29	11.32	18.85
SiK	0.62	1.33	17.74	16.11
MoL	20.71	12.90	368.41	3.34
CrK	19.60	22.54	506.84	2.44
MnK	0.55	0.60	12.95	21.57
FeK	20.33	21.76	420.30	2.77
CoK	18.99	19.26	345.29	2.67
NiK	18.12	18.45	303.09	2.96

b)

Element	Weight %	Atomic %	Net Int.	Error %
O K	0.50	1.81	6.44	25.34
AlK	0.41	0.89	7.68	24.34
SiK	0.58	1.20	15.91	17.55
MoL	13.52	8.22	236.93	3.82
CrK	19.18	21.50	508.88	2.33
FeK	21.73	22.68	458.33	2.56
CoK	21.98	21.74	405.23	2.50
NiK	22.10	21.94	372.10	2.69

c)

Fig. 11. EDS analysis performed in the transition zone from the cladded layer to substrate (Fig. 10): a) elements spectrum; b) chemical composition in Spot 1; c) chemical composition in Spot 2

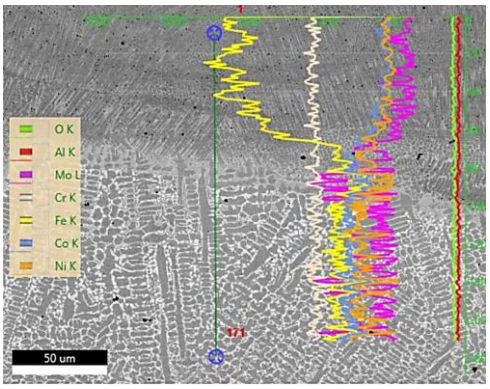

Fig. 12. Distribution of chemical elements on the line crossing the cladded layer - HEA substrate interface

4. CONCLUSIONS

Based on the research results, significant conclusions, in terms of metal-ceramic powders deposited by laser cladding, have been drawn, as follows:

- It was found that using 30% Al_2O_3 ceramic powder dispersed in 70%SS304 metal matrix, best aspect and adhesion of the deposits to the SS304 substrate have been achieved.
- The laser processing parameters – laser power, laser cladding speed – have crucial influence in obtaining continuous and defect-free deposits.
- For identical laser cladding parameters, the use of In718 alloy powders determines larger width of cladded layers, comparing to the SS304 powders.
- Due to the higher viscosity of the SS304 alloy, deposits with higher face reinforcement are obtained.
- The optimal cladding conditions that determine uniform deposition of composite powder mixture with height of 0.45 mm are: laser power of 500 W, cladding process speed of 10 mm/s.
- The microstructural analysis, performed by SEM and EDAX techniques, revealed important information on the adhesion of the composite deposits to the high-entropy alloy substrate, grain refinement in the laser-melted area, and formation of a narrow dilution zone, about 20µm, confirming the mutual compatibility of dissimilar materials, characterized by different mechanical, metallurgical, and chemical characteristics.
- Although the laser cladding process is known as a process that operates with high values of speed, the concentrated energy of the laser beam determines mutual diffusion of chemical elements through the cladded layers - substrate interface, and, further good adhesion of the materials investigated.

ACKNOWLEDGEMENTS

This work was supported by the Romanian National Authority for Scientific Research, CNDI–UEFISCDI, through the project number PN-III-P2-2.1-PED-2019-3953, contract 514PED / 2020 „New ceramic layer composite material processed by laser techniques for corrosion and high temperature applications – LASCERHEA", within PNCDI III. This work was also supported by the Romanian Ministry of Research, Innovation and Digitalization under Romanian National Core Program LAPLAS VII-contract no. 30N/2023. We acknowledge the support of the National Interest Infrastructure facility IOSIN – CETAL at INFLPR.

REFERENCES

[1] **Wang X. et al.**, *Microstructure evolution and crystallography of directionally solidified Al2O3/Y3Al5O12 eutectic ceramics prepared by the modified Bridgman method*, Journal of Materials Science & Technology, vol. 35, no. 9, 2019, pp. 1982–1988.
[2] **Su H., Shen Z., Ma W., Liu Y., Zhao D., Guo Y.,** *Comprehensive microstructure regularization mechanism and microstructure–property stability at 1773 K of directionally solidified Al2O3/GdAlO3 eutectic ceramic composite*, Composites Part B: Engineering, vol. 256, 2023, p. 110647.
[3] **Jiang H.et al.,** *Insights into the influence of powder particle shape on forming process and mechanical properties of Al2O3 ceramic fabricated by laser directed energy deposition*, Additive Manufacturing, vol. 81, 2024, p. 103984
[4] **Geambazu L. E., Voiculescu I., Manea C. A., Bololoi R. V.,** *Economic Efficiency of High-Entropy Alloy Corrosion-Resistant Coatings Designed for Geothermal Turbine Blades: A Case Study*, Applied Sciences, vol. 12, no. 14, 2022, p. 7196.
[5] **Wu D., Shi J., Niu F., Ma G., Zhou C., Zhang B.,** *Direct additive manufacturing of melt growth Al2O3-ZrO2 functionally graded ceramics by laser directed energy deposition*, Journal of the European Ceramic Society, vol. 42, no. 6, 2022, pp. 2957–2973.
[6] **Shen Z., et al.,** *Large-size complex-structure ternary eutectic ceramic fabricated using laser powder bed fusion assisted with finite element analysis*, Additive Manufacturing, vol. 72, 2023, p. 103627.
[7] **Su H. et al.,** *One-step preparation of melt-grown Al2O3/GdAlO3/ZrO2 eutectic ceramics with large size and irregular shape by directed energy deposition*, Additive Manufacturing, vol. 70, 2023, p. 103563.
[8] **Barkia B., Aubry P., Haghi-Ashtiani P., Auger T., Gosmain L., Schuster F., Maskrot H.,** *On the origin of the high tensile strength and ductility of additively manufactured 316L stainless steel: Multiscale investigation*Journal of Materials Science & Technology, vol. 41, 2020, pp. 209–218.
[9] **Mihai S., Baciu F., Radu R., Chioibasu D., Popescu A. C.,** *In Situ Fabrication of TiC/Ti–Matrix Composites by Laser Directed Energy Deposition*, Materials, vol. 17, no. 17, 2024, p. 4284.
[10] **Mihai, S., Toma, V., Sima, A., Chioibasu, D., Popescu, A.C.,** *A novel method of non-destructive characterization via X-ray and high-speed imaging of TiC/IN718 composite materials manufactured by LMD*, Results in Engineering, 2024, p. 103350.
[11] **Chioibasu D., Mihai S., Cotrut C. M., Voiculescu I., Popescu A. C.,** *Tribology and corrosion behavior of gray cast iron brake discs coated with Inconel 718 by direct energy deposition*, International Journal of Advanced Manufacturing Technology, vol. 121, no. 7–8, 2022, pp. 5091–5107.
[12] **Mihai S., Chioibasu D., Mahmood M. A., Duta L., Leparoux M., Popescu A. C.,** *Real-Time Defects Analyses Using High-Speed Imaging during Aluminum Magnesium Alloy Laser Welding*, Metals, vol. 11, no. 11, 2021, p. 1877.
[13] **Simion G., Birsan, D., Voiculescu I., Scutelnicu E.,** *Simulation by FEM of TIG Deposition Welding of Multicomponent Alloy on Carbon Steel Substrate*, Acta Technica Napocensis - Series: Applied Mathematics, Mechanics, and Engineering, vol. 67, no. 1s, 2024.
[14] **Fan Z., Zhao Y., Tan Q., Yu B., Zhang M. X., Huang H.,** *New insights into the growth mechanism of 3D-printed Al2O3–Y3Al5O12 binary eutectic composites*, Scripta Materialia, vol. 178, pp. 2020, pp. 274–280.

[15] **Huang, Y. et al.,** *Process optimization of melt growth alumina/aluminum titanate composites directed energy deposition: Effects of scanning speed*, Additive Manufacturing, vol. 35, 2020, p. 101210.
[16] **Fan Z. et al.,** *Unveiling solidification mode transition and crystallographic characteristics in laser 3D-printed Al2O3-ZrO2 eutectic ceramics*, Scripta Materialia, vol. 210, 2022, p. 114433.
[17] **Liu H. et al.,** *Preparation of large-size Al2O3/GdAlO3/ZrO2 ternary eutectic ceramic rod by laser directed energy deposition and its microstructure homogenization mechanism*, Journal of Materials Science & Technology, vol. 85, 2021, pp. 218–223.
[18] **Zhao D., Wu D., Shi J., Niu F., Ma G.,** *Microstructure and mechanical properties of melt-grown alumina-mullite/glass composites fabricated by directed laser deposition*, Journal of Advanced Ceramics, vol. 11, no. 1, 2022, pp. 75–93.
[19] **Su H. et al.,** *Microstructures and mechanical properties of directionally solidified Al2O3/GdAlO3 eutectic ceramic by laser floating zone melting with high temperature gradient*, Journal of the European Ceramic Society, vol. 37, no. 4, 2017, pp. 1617–1626.
[20] **Ye X., Ma M., Cao Y., Liu W., Gu Y.,** *The Property Research on High-entropy Alloy AlxFeCoNiCuCr Coating by Laser Cladding*, Physics Procedia 12, 2011, pp. 303–312.
[21] **Yang, X., Ge, Y., Lehtonen, J., Hannula, S-P.,** *Hierarchical Microstructure of Laser Powder Bed Fusion Produced Face-Centered-Cubic-Structured Equiatomic CrFeNiMn Multicomponent Alloy*, Materials, vol. 13, 20202, p. 4498.
[22] **Voiculescu I., Geanta V., & all.,** *Irradiation and Temperature on Microstructural Characteristic of FeCrAl Alloys*, Acta Physica Polonica A, vol. 134, iss. 1, 2018, pp.116-118.
[23] **Pascu A., Stanciu E. M., Voiculescu I., Țierean M. H., Roata I. C., Ocaña J. L.,** *Chemical and Mechanical Characterisation of AISI 304 and AISI 1010 Laser Welding*, Materials and Manufacturing Processes, vol. 31, iss. 3, 2016, pp. 311-318.
[24] **Huang Y., Ansari M., Asgari H., Farshidianfar M.H., Sarker D., Khamesee M. B., Toyserkani E.,** *Rapid prediction of real-time thermal characteristics, solidification parameters and microstructure in laser directed energy deposition (powder-fed additive manufacturing)*, Journal of Materials Processing Technology, vol. 274, 2019, p. 11628.
[25] **Wu Q., Long W., Zhang L., Zhao H.,** *A review on ceramic coatings prepared by laser cladding technology*, Optics & Laser Technology, vol. 176, 2024, p.110993.
[26] **Li Q., Cui J., Yang Y., Li J., Zhao Y., Yu C., Wang Q., Zhang P.,** *Enhanced surface wettability modification of Al2O3 for laser cladding ceramic-metal composite coatings*, Materials Today Communications, vol. 40, 2024, p.109746.